ARTICLES

Role of the excited electron in the diffusion of interstitials in AgCl and AgBr

Chun-rong Fu and K. S. Song
Physics Department, University of Ottawa, Ottawa, Canada K1N 6N5
(Received 2 June 1998)

The shallow electrons associated with certain impurities or interstitial silver in AgBr and AgCl are believed to play key roles in some of the photoinduced processes. We have performed theoretical calculations on these systems using a method developed earlier for excited electron centers in insulators. In both AgCl and AgBr crystals the Frenkel-pair energies are found to vary monotonously as a function of the vacancy-interstitial separation, which shows the energetical tendency of the interstitial diffusion toward the vacancy. To obtain the very small activation energy of the interstitial silver diffusion, a simple model of quadrupolar deformation of the Ag^+ ion is employed. We found that the barrier for diffusion from the second cell to the vacancy is substantial (e.g., 0.4 eV) compared with a much smaller value far from the vacancy, ≈ 0.07 eV. The role of the excited electron in silver diffusion is studied. Our calculation shows that the electron can be bound to the silver vacancy in a diffuse orbital when an interstitial silver ion is present nearby. The diffuse electron is found to further reduce the activation energy at moderate distance from the vacancy. Moreover, the large barrier in the second cell from the vacancy was significantly reduced by the diffuse electron. Possible mechanisms for the recently observed anomalous heat generation in photoexcited silver halides are presented.
[S0163-1829(99)04004-7]

I. INTRODUCTION

In silver halides, there are well-known shallow electron centers associated with Cd^{2+} and other divalent ions,[1] or with interstitial silver ions.[2] As the clustering of interstitial silver ions into the formation of latent image is mediated by conduction electrons, the role of shallow electron traps is very important. The defect or impurity-trapped electrons are generally considered to be in a shallow state, often described by the effective mass approaches.[1,2] Recent work by Kondo, Goto, and Sakaida[3] has shown that in silver chloride and bromide crystals, an anomalous amount of heat is generated after photoexcitation, and the effect lasts up to about ten hours after the band-gap excitation has been terminated. They attributed it to the silver interstitial migration toward the cation vacancies mediated by excited electrons. In other words, the excited electron assists in the recombination of Frenkel defect pairs in the cation sublattice with high efficiency.

Reviews[4,5] of various experimental data have indicated the predominant defects in AgCl and AgBr are the Frenkel pairs, consisting of interstitial silver ions and vacancies. Ionic conductivity measurements and analyses have also indicated that the interstitial silver ion has the dominant mobility in AgCl with an activation energy for motion of 0.02–0.04 eV. The reasons for the low activation energy for mobility are thought to be related to the high polarizability of the silver ion in the lattice. This was demonstrated in the modeling studies of silver ion mobility in AgCl by Jacobs and co-workers.[6] Only with the inclusion of quadrupolar deformation of the silver ion from spherical symmetry could the low activation energy for mobility be explained. Likewise, studies of the phonon dispersion required the inclusion of this deformability to reproduce experimental dispersions.[7,8] These studies clearly display the complicated behavior of silver ions in silver halides.

In this paper we present a theoretical study on the role of an excited electron in mediating the diffusion of the interstitial silver ions. The method we used is the same as those developed earlier[9,10] in the studies of the self-trapped excitons in rare gas solids and ionic halides. A few electrons (usually the excited electron) are treated in the Hartree-Fock approximation and the lattice and polarization are treated, respectively, by the classical pair potentials and point polarizable dipole approaches. In evaluating the electronic energies of the diffuse state, the contribution of a large number of ions (about 8000) is taken into account. A limited number of atoms, typically in the range of about 85, are explicitly relaxed to new equilibrium position one at a time by evaluating the gradient of the total energy of the system. Details of the method are given in Refs. 9 and 10. This is similar to the approach used in a recent molecular dynamics study of excited ionic halide clusters.[11]

The main results of our work are as follows. (1) In the absence of an excited electron, there is a monotonous decrease of the total energy as a function of vacancy-interstitial distance up to the second cell separation. The potential barrier between adjacent nearest-neighboring separations, e.g., the third and fourth vacancy interstitial, is about 0.07 eV. However, in the last stage of diffusion the barrier rises to a much higher value (about 0.37 eV and 0.39 eV, respectively, for AgCl and AgBr). (2) An excited electron is found to bind at the silver vacancy in a diffuse orbital [$\alpha < 0.0075$ (atomic units) in Gaussian base $\exp(-\alpha r^2)$], although the more

TABLE I. Pair potential coefficients. A, ρ, C are in atomic units.

Coefficient	Ag^+-Ag^+	Ag^+-Cl^-	Cl^--Cl^-	Ag^+-Br^-	Br^--Br^-
A	607.39	92.56	45.10	111.61	108.34
ρ	0.4479	0.6180	0.6073	0.6111	0.6274
C	374.88	367.38	125.52	382.22	207.52

compact state is nonbinding ($\alpha > 0.015$). This electron is found to lower the barrier height somewhat even at larger separation. (3) The diffuse electron has the most important influence on the nearest-neighboring Frenkel pair and the barrier height is reduced from about 0.4 eV to about 0.05 eV. (4) Both the vacancy-diffusion and collinear interstitialcy mechanisms are effective in the last leg of interstitial Ag^+ diffusion toward the vacancy. The results seem to be able to explain the observed heat generation reported by Kondo, Goto, and Sakaida.[3]

This paper is organized in the following manner. In Sec. II, the theoretical method employed is briefly described, and appropriate parameters used are given and discussed. Section III presents the interstitial Ag^+ diffusion toward the vacancy in the absence of the excited electron, then the effect of the excited electron on the interstitial diffusion is described. Section IV concludes this work.

II. METHOD OF CALCULATION

A. Pair potential

The pair potential used is of the Buckingham form:

$$V_{ij} = A_{ij}\exp(-r/\rho_{ij}) - C_{ij}/r^6. \tag{1}$$

There is a large van der Waals attractive term between the Ag^+ cations as was described in Ref. 12. This attractive term has the effect of stabilizing the cation interstitials and so accounts for the low Frenkel defect formation energy compared to that for the alkali halides. The parameters A_{ij}, ρ_{ij}, and C_{ij} taken from Ref. 12 are listed in Table I.

B. Polarization energy

We assumed that the ions behave as point dipoles with polarizability equal to the free atomic polarizability. This is acceptable when the overlap between neighboring ions is small.

The polarization energy is expressed as

$$E_{\rm pol} = -\sum_i \vec{\mu}(\vec{R}_i)\cdot\vec{E}(\vec{R}_i), \tag{2}$$

$$\vec{\mu}(\vec{R}_i) = \alpha_i \vec{E}(\vec{R}_i), \tag{3}$$

where $\vec{E}(\vec{R}_i)$ is the local electric field produced by the defect electron and the lattice distortion. $\vec{\mu}(\vec{R}_i)$ is the dipole moment induced on the ion at $\vec{R}_i$. α_i is the free atomic polarizability of ion i.

However, in silver halides the overlap between neighboring ions is not negligible. Because of the importance of the polarization energy in the determination of the relaxed system we decided to scale the polarization energy by a parameter ξ so that the calculated Frenkel-pair formation energy agreed with experimental data [1.4 eV for AgCl and 1.1 eV for AgBr (Ref. 13), i.e.,

$$E_{\rm pol}^{\rm rel} = \xi E_{\rm pol}. \tag{4}$$

The optimized ξ was found to be 0.65 for AgCl, and 0.59 for AgBr, respectively.

The polarizabilities used in the present work are 1.888 $Å^3$ for Ag^+, 2.947 $Å^3$ for Cl^-, and 4.091 $Å^3$ for Br^-.[13]

C. Treatment of the excited electron

We have developed earlier a package of methods to determine the structure and energetics of defects in insultating crystals containing one or two excess electrons. The interaction of the electron with the deep core orbital of the lattice ions is treated with the ion-size parameters originally formulated by Bartram, Stoneham, and Gash[14] and Zwicker,[15] while the outer s, p, and d orbitals are calculated directly through interpolation formulas. The use of a floating 1s Gaussian orbital (FGO) makes it practical to evaluate various short-range terms (screened Coulomb, exchange, and overlap integrals) efficiently. It also gives us the flexibility of placing the Gaussians at appropriate positions in the crystal to best represent the defect electron states.

The Hamiltonian of the system is given as

$$H = -\frac{1}{2}\Delta^2 + V_{\rm PI}(\vec{r}) + V_{\rm SC}(\vec{r}) + V_{\rm EX}(\vec{r}), \tag{5}$$

where $V_{\rm PI}$, $V_{\rm SC}$, and $V_{\rm EX}$ are point ion potential, screened Coulomb potential and exchange potential, respectively.

The defect electron wave function is represented by Ψ, which is orthogonal to all the ionic orbitals $\chi_{\gamma,\lambda}$. $\chi_{\gamma,\lambda}$ is the λth occupied atomic orbital on the γth atom.

$$|\Psi\rangle = \sum_i c_i \left(|\phi_i\rangle - \sum_{\gamma,\lambda} |\chi_{\gamma,\lambda}\rangle\langle\chi_{\gamma,\lambda}|\phi_i\rangle \right), \tag{6}$$

where ϕ_i is a floating 1s Gaussian ($\exp[-\alpha_i(\vec{r}-\vec{R}_i)^2]$). Either Gaussians at different positions or different Gaussians at the same position are used in the linear combination. The problem now is solving the secular equation for the state Ψ and its energy E:

$$|H_{i,j} - ES_{i,j}| = 0. \tag{7}$$

With the introduction of the ion-size parameters for deep core and the interpolation formulas for the short-range energy terms and overlap integrals, we can easily obtain the system energy and further determine the equilibrium configuration by minimizing the total energy with respect to the relaxation of ions. The detailed expressions and corresponding parameters are given in the Appendix.

The lattice configuration is optimized by minimizing the total energy ($E_{\rm total}$) which is the sum of the lattice Coulomb energy ($E_{\rm Coul}$), the lattice repulsive energy ($E_{\rm rep}$), the polarization energy ($E_{\rm pol}$) and the excited electron energy ($E_{\rm elec}$):

$$E_{\rm total} = E_{\rm Coul} + E_{\rm rep} + E_{\rm pol} + E_{\rm elec}. \tag{8}$$

TABLE II. Frenkel-pair energies (eV) at different separations. The vacancy is at (0,0,0), interstitial at (x,0.5,0.5) in units of the half lattice constant a.

x	0.5	1.5	2.5	3.5	4.5	5.5	6.5	7.5	∞
E_f (AgCl)	0.589	0.486	0.487	0.503	0.567	0.651	0.729	0.808	1.430
E_f (AgBr)	0.490	0.269	0.301	0.323	0.366	0.444	0.560	0.620	1.155

In practice we calculated the energy gradients for individual ions, then all movable ions were placed at the new positions. This cycle was repeated until the total energy change is within a specified value (here it is set at 0.005 eV).

III. RESULTS AND DISCUSSION

A. Frenkel-pair energy

With the optimized scaling parameters ξ for polarization energy, the calculated formation energies of a Frenkel pair are 1.43 eV for AgCl and 1.16 eV for AgBr. The Frenkel-pair energies in various separations are also given in Table II.

One can easily see that starting from the second cell the Frenkel-pair energy varies monotonously as a function of the interstitial-vacancy separation. Therefore the interstitial ion $(Ag^+)_i$ has the energetical tendency to diffuse toward the vacancy.

B. Quadrupolar deformation

It has been shown by Kleppmann[17] and Jacobs and co-workers[6] that the deformation of the Ag^+ is an important factor in determining the very small migration energy in silver halides. As the mobile Ag^+ ion approaches the collinear interstitialcy (ic) saddle point it must pass through the center of an equilateral triangle of the three Cl^- (Br^-) ions 1, 2, and 3 (see Fig. 1). Clearly the overlap can be reduced by the outward movement of the nearest Cl^- (Br^-) ions, and in the alkali halides this is the only mechanism of reducing the repulsive energy in the saddle point. However, the activation energy for Ag^+ migration is so small that the rearrangement of the surrounding ions can never gain enough energy to lower the barrier to about 0.1 eV. A further reduction in overlap can only be achieved by the deformation of the Ag^+ ion. In this work we adopted the quadrupolar deformation model proposed in Ref. 6. The assumed deformation is that the mobile Ag^+ ions are elongated along the migration direction by $2h$ and contracted symmetrically by h in the plane normal to the direction of motion. The shape of the ion is thus an ellipsoid of revolution. The short-range interaction between any two ions (deformed or not) whose centers are at a distance r apart can be calculated from the pair potential using an effective interaction distance r_e defined by[6]

$$r_e = r + \delta r_1 + \delta r_2, \tag{9}$$

where

$$\delta r_i = r_{i,s} - r_i. \tag{10}$$

$r_{i,s}$ is the radius of the original spherical ion and r_i is the radius vector of the first ion in the direction to the second; it thereby depends on the quadrupolar deformation.

In Ref. 6 the barrier is assumed to occur at the configuration in which the two mobile Ag^+ ions are just located at their own saddle points simultaneously. The activation energy was then evaluated by taking the difference between the energies of this barrier configuration and the reference configuration, which holds an interstitial silver ion at cubic center and other ions at normal sites. It is easily understood that the repulsive interaction of the mobile Ag^+ ion with its three nearest Cl^- ions reaches the maximum at the saddle point. Therefore, when one Ag^+ ion is at its saddle point, the second Ag^+ ion must relax to a certain position in the path which may not be its own saddle point in general. This means that the two Ag^+ ions can reach their own saddle points separately. To simulate the migration of the Ag^+ ions the change in the deformation at different positions should be taken into account. We propose the following approximate formula to model the deformation along the migration path:

$$h = \frac{h_0}{r_0^2} r(2r_0 - r) e^{-\eta(r - r_s)^2}, \tag{11}$$

where $r_0 = \sqrt{3}a/4$ (a is the nearest-neighbor distance) is the half length of the path, which starts from the interstitial position (cubic center) and ends at the regular site or conversely; r_s is the distance between the geometrical saddle point and the starting position of the mobile ion. $r_s = r_0/3$ when starting position is an interstitial, or $r_s = 2r_0/3$ when starting position is a regular site; r is the moving distance of the Ag^+ ion. The polynomial $r(2r_0 - r)$ is introduced to en-

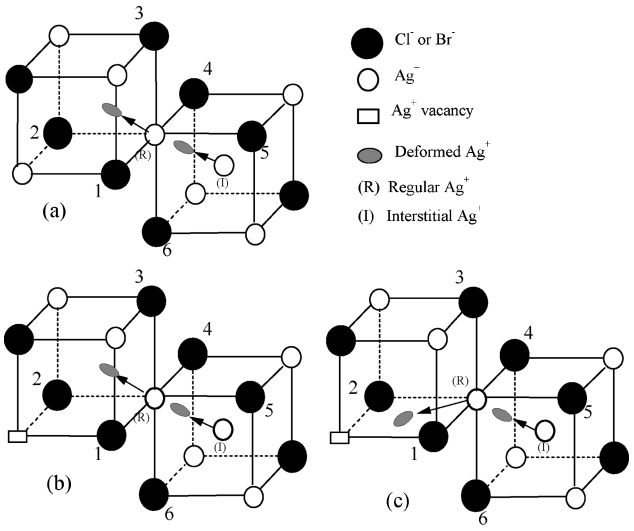

FIG. 1. The migration diagrams of two deformed silver ions in AgCl or AgBr crystal. (a) Diffusion far from the vacancy via collinear interstitialcy mechanism. (b) Diffusion from the cell next to the vacancy via collinear interstitialcy path. (c) Diffusion from the cell next to the vacancy via vacancy-diffusion mechanism.

TABLE III. The barrier configuration and activation energy for AgCl and AgBr in the region far from the vacancy. Coordinates are in units of a.

Type	Coordinates of $(Ag^+)_i$ and $(Ag^+)_r$		Energy terms (eV)				Activation
	$(Ag^+)_i$	$(Ag^+)_r$	E_{Coul}	E_{rep}	E_{pol}	E_{total}	Energy (eV)
AgCl	(3.17 0.17 0.83)	(2.65 −0.35 1.35)	5.330	0.909	−5.670	0.570	0.067
	Reference energy		5.879	0.482	−5.857	0.503	
AgBr	(3.33 0.33 0.67)	(2.83 −0.17 1.17)	4.638	1.400	−5.659	0.380	0.057
	Reference energy		5.614	0.527	−5.818	0.323	

sure that the deformation is zero at the regular site or at the interstitial according to the symmetry, and the Gaussian function is used to control the rate of deformation in the path. The two parameters h_0 and η can be adjusted to obtain the desired deformation and yield a reasonable migration energy. In this work we have used $h_0=0.068a$ and $\eta=0.25$ for AgCl, $h_0=0.070a$ and $\eta=0.22$ for AgBr.

The Ag^+ ion cannot deform without limit because of the additional quadrupolar energy, which yields[6]

$$E_Q=\frac{3}{2}K_Q h^2 \tag{12}$$

per deformed ion. K_Q is the anharmonic quadrupolar force constant which, following Kleppmann,[17] is taken to be

$$K_Q=K_{Q_0}[1-(2h/r_{Ag^+})]^{-2}, \tag{13}$$

where r_{Ag^+} is the radius of Ag^+ which equals 1.26 Å,[13] and the optimized value for K_{Q_0} is 0.60 eV Å^{-2}.

C. Migration of interstitial Ag^+ without electron

There are two possible interstitialcy diffusion mechanisms of $(Ag^+)_i$ ion considered here; the first is collinear (ic), as shown in Fig. 1(a), and the second noncollinear ($i$nc). In the first mechanism the interstitial Ag^+ ion moves along the diagonal direction to push one of its nearest-neighboring Ag^+ ions on a regular lattice site into another interstitial position and itself occupies the lattice site of the displaced Ag^+ ion. During diffusion the two ions jump in the same direction. In the second mechanism the two mobile Ag^+ ions move in different diagonal directions. Our calculation shows that the noncollinear interstitialcy path always gives a much higher barrier than the collinear one in the region far from the vacancy, therefore we have dropped this mechanism for now. However, the situation is quite different when the interstitial silver ion is close to the vacancy. The so-called vacancy diffusion mechanism [see Fig. 1(c)] also gives a barrier comparable to that of the collinear path.

We first discuss the ic migration of the interstitial in the region far from the vacancy, which is placed at the origin of the coordinate system. Without loss of generality, the interstitial Ag^+ ion, denoted by $(Ag^+)_i$, is taken to be in the third cell from the vacancy with the coordinates (3.5,0.5, 0.5). It then diffuses along the direction $[-1,-1,+1]$, i.e., towards the silver ion at regular site (3.0,0.0,1.0) [see Fig. 1(a)]. This regular Ag^+ ion, denoted by $(Ag^+)_r$, will simultaneously move in the same direction $[-1,-1,+1]$ as the interstitial silver ion does. Therefore the diffusion path for $(Ag^+)_i$ is from (3.5,0.5,0.5) to (3.0,0.0,1.0), while for $(Ag^+)_r$ it is from (3.0,0.0,1.0) to (2.5,−0.5,1.5). In practice we fix one Ag^+ ion in discrete positions and let the second ion relax along the path to reach the minimum of system energy. The calculation shows that the barrier always appears when one of the mobile Ag^+ ions is at the geometrical saddle point, and the barrier height greatly depends on the deformation of the mobile Ag^+ ions. With $h_0=0.068a$ (a is the shortest anion-cation distance) for AgCl, the calculated activation energy is about 67 meV for AgCl, which compares reasonably well with the experimental value. The detailed results are given in Table III.

Here the reference energy is obtained by full lattice optimization when the interstitial silver ion $(Ag^+)_i$ is at the cubic center (3.5, 0.5, 0.5) and other ions at normal sites. One can find in Table III that in AgCl the barrier occurs when $(Ag^+)_r$ is at the geometrical saddle point, i.e., the center of the triangle formed by the three Cl^- ions 1, 2, and 3, as shown in Fig. 1(a), and the $(Ag^+)_i$ relaxes to a position very close to the regular site (3.0, 0.0 1.0). In AgBr the barrier appears when $(Ag^+)_i$ is at the saddle point which is the center of the triangle formed by three Br^- ions 4, 5, and 6. As the ions Cl^- and Br^- differ in polarizability and ion size, the barrier configurations in these two systems are different. However, in either of the two cases, there is always one mobile Ag^+ at the geometrical saddle point. In this regard our result is different from that of Jacobs and co-workers.[6] They assumed the two Ag^+ ions are simultaneously at their respective saddle points. We also calculated the energies for such configurations, which are 0.71 eV for AgCl and 0.53 eV for AgBr. These energies are obviously higher than the configurations listed in Table III. Therefore it is unlikely for the second mobile silver ion to occupy its own saddle point while the first one is at the corresponding saddle point. Another interesting feature is that the two mobile Ag^+ ions keep almost the same separation during the collinear migration course, which is about 2.49 Å for AgCl and 2.50 Å for AgBr, respectively. Considering the Ag^+ radius is about 1.26 Å,[13] the two mobile Ag^+ ions behave like a molecule in the collinear interstitialcy diffusion. This is somewhat like in the so-called split interstitial,[16] which consists of a pair of Ag^+ with a bound electron located at a single lattice site. Further calculation shows that the activation energy in the region far from the vacancy is always smaller than 0.07 eV for both AgCl and AgBr.

In the region close to the vacancy, some new features emerge. To have a collinear interstitial diffusion path, the reference configuration has been chosen with the interstitial Ag^+ at (1.5,1.5,−0.5) so that this interstitial Ag^+ and the regular Ag^+ at (1.0,1.0,0) can move along the $[-1,-1,$

TABLE IV. The barrier configuration and activation energy for AgCl and AgBr in the region close to the vacancy (collinear interstitialcy migration).

Type	Coordinates of $(Ag^+)_i$ and $(Ag^+)_r$ $(Ag^+)_i$	$(Ag^+)_r$	E_{Coul}	E_{rep}	E_{pol}	E_{total}	Activation Energy (eV)
AgCl	(1.21 1.21 −0.21)	(0.67 0.67 0.33)	4.223	1.080	−4.481	0.821	0.365
	Reference energy [a]		6.243	0.110	−5.897	0.456	
AgBr	(1.21 1.21 −0.21)	(0.67 0.67 0.33)	2.354	1.594	−3.277	0.672	0.389
	Reference energy [a]		5.431	0.462	−5.610	0.283	

[a]The reference energies are calculated when interstitial Ag^+ is at (1.5,1.5,−0.5).

+1] direction. After diffusion, the $(Ag^+)_r$ at (1.0,1.0,0) reaches the interstitial position (0.5,0.5,0.5) and becomes the new interstitial $(Ag^+)_i$, while the original $(Ag^+)_i$ occupies the vacated lattice site (1.0,1.0,0). Another mechanism is the so-called vacancy mechanism, in which the $(Ag^+)_r$ at (1.0, 1.0, 0) moves along the direction [−1,−1,0] toward the vacancy and finally recombines with the vacancy, while the original $(Ag^+)_i$ moves to the (1.0, 1.0, 0) site. The two diffusion mechanisms are illustrated in Figs. 1(b) and 1(c). The system energy of the reference configuration was found to be 0.46 eV for AgCl and 0.28 eV for AgBr, respectively. These energies are lower than when the interstitial Ag^+ is at the cubic center of the central cell, i.e., (0.5,0.5,0.5), which is, respectively, 0.59 eV for AgCl and 0.49 eV for AgBr (see Table II). Therefore in the region close to the vacancy the activation energy must be substantial compared with the small value far away from the vacancy. The calculated results for the above two mechanisms are listed in Table IV and Table V.

Here the same deformation parameters as in the region far from the vacancy have been used to calculate the barriers. Obviously the activation energy is much higher near the central cell than in the region far from the vacancy. The reason resulting in this large barrier is mainly due to the lattice compression around the vacancy at (0,0,0). By comparing the repulsive energies in Table IV and Table III, one can find that for AgCl the repulsive energy difference between the reference configuration and barrier configuration is 0.97 eV in the central region, but only 0.43 eV in the far away region. A similar situation happens to AgBr, too. As there have been no experimental results reported for the collinear activation energy near the central cell, we are not able to make accurate comparisons. Although the calculation can be refined by optimizing the deformation parameters, the purpose of this work is to study the effect of the defect electron on the diffusion of the interstitial Ag^+ ion rather than to simulate precisely the defect migration. Therefore, the above results are adequate to demonstrate the behavior of the mobile Ag^+ ions along the different paths. It is worth mentioning that once the $(Ag^+)_r$ at (1.0,1.0,0) moves to the interstitial position (0.5, 0.5,0.5) in the collinear path or position (0.5, 0.5, 0) in the vacancy-diffusion path, it diffuses freely toward the vacancy and recombines with it.

D. Effect of the excited electron

Shallow electron centers in silver halides are created upon optical excitation and are believed to play an important role in the latent image formation process. It was suggested that the intrinsic binding core consists of an interstitial ion,[1] but other models include a substitutional silver ion at a surface kink or an internal jog.[18] Recently, the first electron-nuclear double resonance (ENDOR) spectrum of intrinsic shallow electron centers in AgCl was used to determine the spatial delocalization of the loosely bound electron.[2] A model is suggested in which an electron is weakly trapped by two adjacent silver ions on a single cationic site. All these works indicate that a shallow electron is associated with the interstitial silver ion. Kondo and his co-workers have adopted these models to explain the anomalous heat generation in AgCl and AgBr single crystals.[3] They proposed that the trapped electron at an interstitial may screen the interaction with the surrounding ions and therefore lower the activation energy of interstitial migration. It is an interesting problem how the shallow electron actually helps the interstitial silver ion to migrate in the crystal.

We have investigated the interstitial migration by using the above two models, i.e., the electron is either trapped by the interstitial silver ion or bound to the split-interstitial center. For the first model, we have calculated the potential energy curve using different basis sets. Several Gaussians centered on different positions along the diffusing path have been tried (with $\alpha \leqslant 0.010$). Also, a single Gaussian on the diffusing silver interstitial ($\alpha \leqslant 0.010$) has been tried. In all cases, we found that the electron does not induce the lowering of the barrier height. The results turned out to be the

TABLE V. The barrier configuration and activation energy for AgCl and AgBr in the region close to the vacancy (vacancy-diffusion mechanism).

Type	Coordinates of $(Ag^+)_i$ and $(Ag^+)_r$ $(Ag^+)_i$	$(Ag^+)_r$	E_{Coul}	E_{rep}	E_{pol}	E_{total}	Activation Energy (eV)
AgCl	(1.21 1.21 $\overline{0.21}$)	(0.50 0.50 0.00)	2.475	1.278	−2.820	0.932	0.476
AgBr	(1.08 1.08 $\overline{0.08}$)	(0.50 0.50 0.00)	1.550	1.508	−2.213	0.846	0.563

TABLE VI. The barrier configuration and activation energy with electron in the region far from the vacancy (collinear interstitialcy migration).

Type	Coordinates of $(Ag^+)_i$ and $(Ag^+)_r$ $(Ag^+)_i$	$(Ag^+)_r$	Energy terms (eV) E_{Coul}	E_{rep}	E_{elec}	E_{pol}	E_{total}	Activation Energy (eV)
AgCl	(3.21 0.21 0.79)	(2.67 −0.33 1.33)	7.617	0.363	−3.493	−9.188	−4.701	0.050
	Reference energy [a]		8.878	−0.385	−3.296	−9.948	−4.751	
AgBr	(3.33 0.33 0.67)	(2.81 −0.19 1.19)	6.399	1.041	−4.497	−8.328	−5.385	0.039
	Reference energy [a]		7.013	0.300	−4.364	−8.373	−5.424	

[a]The reference energies are calculated when interstitial Ag^+ is at (3.5,0.5,0.5).

opposite of our initial expectation. This can be explained in the following way: The electronic energy rises at the saddle point compared with its regular interstitial position because the electron center gets closer to the three Cl^- or Br^- ions 4, 5, and 6 [see Fig. 1(a)]. Besides, the polarization of the local cluster becomes slightly weaker due to the screening effect of the electron. While the repulsive potential, which is the dominant part of the barrier, is not significantly influenced by the presence of the electron, the activation energy in this model is therefore larger than without the electron. The second model, in which the electron is represented by a single Gaussian centered on the midpoint between the interstitial and the regular moving silver ion, leads to a similar conclusion. Overall, our detailed calculations seem to indicate that the conduction electron cannot assist the interstitial diffusion by binding to the interstitial.

As it turned out, the excited electron can reduce the activation energy when it is bound at the silver vacancy in a diffuse orbital. Especially, it makes a crucial contribution to the Ag^+ migration in the last stage of diffusion toward the vacancy. The cation vacancy has an effective negative point charge. The interaction between the cation vacancy and electron is always a repulsive one. It is true that a pure cation vacancy (''pure'' means there is no interstitial near the vacancy) cannot be a trapping center of an electron. However, the situation is different with an interstitial available in the system, especially when the interstitial is close to the vacancy. In this case, the net background charge is zero. Therefore the electron could be loosely trapped at the vacancy due to the attractive interaction of polarization and exchange effects. We found that the optimized Gaussian base is less than 0.0075 a.u., depending on the separation between the interstitial and vacancy. The larger the separation, the shallower the electron. We have used an optimized Gaussian 0.0072 for AgCl and 0.0052 for AgBr in this work, with the mean radius 5.0 and 5.9 Å, respectively. This single Gaussian is centered on the vacancy.

In the region away from the vacancy we found that the shallow electron trapped at the vacancy can still lower the barrier height if the distance is modest, as shown in Table VI. In this case, the overlap of the diffuse wave function of the shallow electron with the interstitial silver is not negligible. The results in Table VI are calculated under the same lattice configurations as in Table III. The barrier height decreases by about 0.02 eV in both AgCl and AgBr.

In the nearest-neighboring cell the electron plays an even more important role. The results in the preceding subsection indicated that without the electron the activation energy in the last stage of diffusion is over 0.30 eV for interstitialcy migration and even higher for vacancy diffusion. With such a large barrier, it is almost impossible for the interstitial to recombine with the vacancy. However, the shallow electron trapped at the vacancy helps to lower the barrier significantly in this step of diffusion. The detailed results are presented in Table VII and Table VIII.

Comparing Tables VII and VIII with Tables IV and V, one can see that the barriers for both collinear interstitialcy migration and vacancy diffusion have almost been removed by the electron. The barrier mainly results from the repulsive interaction of the Ag^+ ion with three Cl^- or Br^- ions 1, 2, and 3. When the electron is trapped at the vacancy, the repulsive energy dropped from 1.080 to 0.691 eV for AgCl, and from 1.594 to 0.886 eV for AgBr in the collinear mechanism. It also decreased by about 0.47 eV in the vacancy-diffusion mechanism for both AgCl and AgBr. The decrease in the repulsive energy at the saddle point indicates that the local lattice surrounding the mobile Ag^+ ions has expanded. By examining the lattice distortion field, we found that the anions 1 and 2 experienced a small displacement (about 0.09 Å) with the electron at the vacancy, while without the electron the displacement is 0.23 Å inward. These two ions play the most important role in forming the barrier. Now that the electron can repel them to move away from the $(Ag^+)_r$

TABLE VII. The barrier configuration and activation energy with electron in the region close to the vacancy (collinear interstitialcy migration).

Type	Coordinates of $(Ag^+)_i$ and $(Ag^+)_r$ $(Ag^+)_i$	$(Ag^+)_r$	Energy terms (eV) E_{Coul}	E_{rep}	E_{elec}	E_{pol}	E_{total}	Activation Energy (eV)
AgCl	(1.17 1.17 −0.17)	(0.67 0.67 0.33)	6.869	0.691	−5.023	−7.541	−5.004	0.018
	Reference energy [a]		8.353	−0.497	−4.114	−8.764	−5.022	
AgBr	(1.17 1.17 −0.17)	(0.67 0.67 0.33)	5.771	0.886	−6.050	−6.358	−5.751	0.012
	Reference energy		7.431	−0.025	−5.244	−7.925	−5.763	

[a]The reference energies are calculated when interstitial Ag^+ is at $(1.5,1.5,\overline{0.5})$.

TABLE VIII. The barrier configuration and activation energy for AgCl and AgBr in the region close to the vacancy (vacancy-diffusion mechanism).

Type	Coordinates of $(Ag^+)_i$ and $(Ag^+)_r$ $(Ag^+)_i$	$(Ag^+)_r$	Energy terms (eV) E_{Coul}	E_{rep}	E_{elec}	E_{pol}	E_{total}	Activation Energy (eV)
AgCl	(1.06 1.06 $\overline{0.06}$)	(0.50 0.50 0.00)	5.119	0.801	−5.475	−5.427	−4.982	0.040
AgBr	(1.06 1.06 $\overline{0.06}$)	(0.50 0.50 0.00)	3.488	1.040	−6.338	−3.900	−5.709	0.054

ion, the barrier certainly becomes smaller. The repulsive interaction between the electron and the nearest-neighboring anions results mainly from the Coulomb energy. After passing the barrier, the two mobile silver ions can move freely toward the corresponding vacancies and recombine with them.

One may have noted that the electron is more diffuse in AgBr ($\alpha=0.0052$) than in AgCl ($\alpha=0.0072$), which means the electron in AgBr can easily escape the trapping center so as to mediate the recombination of more Frenkel pairs. This is in accordance with the result that the heat generation is more efficient in AgBr than in AgCl.[3]

IV. CONCLUSION

The role of the excited electron in the diffusion of interstitial silver in AgCl and AgBr is studied. We found that the electron can be bound to a silver vacancy in a diffuse orbital when an interstitial is present nearby. This shallow electron enhances the silver interstitial diffusion toward the vacancy generally. The most important role of the electron is to greatly reduce the large barrier encountered by the interstitial in the cell next to the vacancy. Our calculation seems to indicate that an electron trapped at an interstitial does not induce a lowering of the barrier height. The diffusion mechanisms are also discussed in this work. It is found that in the region far from the vacancy the collinear interstitialcy migration has much smaller activation energy than noncollinear diffusion. However, when the interstitial reaches the second cell the vacancy-diffusion mechanism leads to a barrier comparable to that of the collinear path. Therefore in this region both mechanisms are considered for diffusion with and without an electron.

Based on the present work, we propose a mechanism to explain the anomalous heat generation in AgCl and AgBr. Due to the energetic gradient pointing toward the vacancy the interstitial silver ion can diffuse easily with modest thermal activation energy until the cell next to the vacancy is reached. At this point, however, a substantial potential barrier prevents the recombination of the silver interstitial with the vacancy. A photoexcited electron loosely bound to the silver vacancy significantly reduces this barrier. The interstitial silver ion then recombines with the vacancy nonradiatively and releases the Frenkel-pair formation energy to the lattice in the form of heat. After recombination, the shallow electron becomes free again until it captures another interstitial silver ion. Therefore the vacancy-interstitial recombination can be carried on repeatedly as long as the conduction electrons and the silver Frenkel pairs are available in the crystal.

APPENDIX A:

The matrix elements of Hamiltonian and overlap integral can be expressed as follows:

$$H_{ij}=\langle\phi_i|T|\phi_j\rangle+\langle\phi_i|V_{PI}(\vec{r})|\phi_j\rangle+\langle\phi_i|V_{SC}(\vec{r})+V_{EX}(\vec{r})|\phi_j\rangle-\sum_{\gamma,\lambda}(E^0_{\gamma,\lambda}+\Delta E_\gamma)\langle\phi_i|\chi_{\gamma,\lambda}\rangle\langle\chi_{\gamma,\lambda}|\phi_j\rangle \quad \text{(A1)}$$

and

$$S_{ij}=\langle\phi_i|\phi_j\rangle-\sum_{\gamma,\lambda}\langle\phi_i|\chi_{\gamma,\lambda}\rangle\langle\chi_{\gamma,\lambda}|\phi_j\rangle. \quad \text{(A2)}$$

Here we have used Eq. (5) and

$$\langle\chi_{\gamma',\lambda'}|\chi_{\gamma,\lambda}\rangle=\delta_{\gamma\gamma'}\delta_{\lambda\lambda'} \quad \text{(A3)}$$

as well as

$$H|\chi_{\gamma,\lambda}\rangle=E_{\gamma,\lambda}|\chi_{\gamma,\lambda}\rangle=(E^0_{\gamma,\lambda}+\Delta E_\gamma)|\chi_{\gamma,\lambda}\rangle. \quad \text{(A4)}$$

Equations (A3) and (A4) are based on the approximation that there is no overlap between cores on different ions. Here $E_{\gamma,\lambda}$ is the energy of the λth core orbital on the γth atom. It is the free atomic core energy $E^0_{\gamma,\lambda}$ (e.g., taken from the Clementi Roetti table,[19]) shifted by the point-ion potential produced by the rest of the lattice ΔE_γ.

After some manipulation, the two lowest order ion-size terms can be expressed as

$$\sum_{\gamma,\lambda}\langle\phi_i|\chi_{\gamma,\lambda}\rangle\langle\chi_{\gamma,\lambda}|\phi_j\rangle=\sum_\gamma(f_1B_\gamma+f_2K'_\gamma+f_3K_\gamma), \quad \text{(A5)}$$

$$\langle\phi_i|V_{SC}(\vec{r})+V_{EX}(\vec{r})|\phi_j\rangle-\sum_{\gamma,\lambda}(E^0_{\gamma,\lambda}+\Delta E_\gamma)\langle\phi_i|\chi_{\gamma,\lambda}\rangle\langle\chi_{\gamma,\lambda}|\phi_j\rangle=\sum_\gamma(f_1A_\gamma+f_2J'_\gamma+f_3J_\gamma)$$

TABLE IX. Deep core ion-size parameters.

Ion	A	B	J	K	J'	k'
Ag^+	38.47326	1.47029	3.14054	0.16224	4.45149	0.18883
Cl^-	26.20500	3.14300	3.59100	0.58700	5.73700	0.67900
Br^-	33.91133	5.01791	8.02950	1.70585	8.75470	1.33958

TABLE X. Short-range potential interpolation parameters.

Ion	β_{SC}	A_{SC}	β_{EX}	A_{EX}
Ag^+	1.04400	−10.77276	0.15440	−0.85956
Cl^-	0.38240	−4.27110	0.25888	−2.51634
Br^-	0.30624	−4.54650	0.19328	−2.02488

$$+\sum_{\gamma}\Delta E_{\gamma}(f_1 B_{\gamma}+f_2 K'_{\gamma}+f_3 K_{\gamma}). \tag{A6}$$

The A, B, J, J', K, K' are the so-called ion-size parameters which are calculated from deep core orbitals of free ions [the summation over λ in Eqs. (A5) and (A6) is restricted to deep core shells only], while the outermost shells are treated by interpolation. The f_1, f_2, and f_3 are expansion terms of the Gaussian ϕ, they are functions depending only on the Gaussians and the vector joining them to the ion site.

The interpolation formulas for screened Coulomb, exchange potential, and overlap integrals fitted to exact values are

$$\langle\phi_i|V_{SC,\gamma}(\vec{r})|\phi_j\rangle=\int\phi_i^*(\vec{r})\frac{A_{SC,\gamma}e^{-\beta_{SC,\gamma}|\vec{r}-\vec{R}_{\gamma}|^2}}{|\vec{r}-\vec{R}_{\gamma}|}\phi_j(\vec{r})d\tau, \tag{A7}$$

$$\langle\phi_i|V_{EX,\gamma}(\vec{r})|\phi_j\rangle=\int\phi_i^*A_{EX,\gamma}e^{-\beta_{EX,\gamma}|\vec{r}-\vec{R}_{\gamma}|^2}d\tau. \tag{A8}$$

TABLE XI. Overlap interpolation parameters.

	Ag^+	Cl^-	Br^-
β_{sovl}	1.90000	0.50000	1.10000
A_{sovl}	0.68115	0.56504	1.40270
κ_s	4.00000	4.00000	8.00000
E_s (eV)	−4.29518	−0.71014	−0.67924
β_{povl}	1.05000	0.37500	0.35000
A_{povl}	0.06572	0.36356	0.44269
κ_p	4.00000	4.00000	5.00000
E_p (eV)	−2.96410	−0.12840	−0.13320
β_{dovl}	0.85000		
A_{dovl}	0.22504		
κ_d	4.00000		
E_d (eV)	−0.82467		

It was found that two Gaussians with their exponents related by a simple ratio could give the overlap integral fits of sufficient accuracy:

$$\langle\phi_i|\chi_x\rangle=N^x\int\phi_i^*(N_1^x e^{-\beta_{xovl}r^2}+A_{xovl}N_2^x e^{-\beta_{xovl}r^2/\kappa_x})d\tau. \tag{A9}$$

Here x denotes the s,p,d orbitals, respectively; κ_x is the ratio of the exponents of the two fitted Gaussians, which is determined together with A_{xovl} and β_{xovl} by the least squares fitting procedure. N_1^x, N_2^x, and N^x are normalization factors.

All the parameters used in this work are listed in Tables IX–XI.

[1] S. Sakuragi and H. Kanzaki, Phys. Rev. Lett. **38**, 1302 (1977).
[2] M. T. Bennebroek, O. G. Poluektov, A. J. Zakrzewski, P. G. Baranov, and J. Schmidt, Phys. Rev. Lett. **74**, 442 (1995).
[3] Y. Kondo, I. Goto, and N. Sakaida, Phys. Rev. B **55**, 9534 (1997).
[4] R. J. Friaut, J. Phys. (France) **38**, 1077 (1977).
[5] R. Friauf, *The Physics of Latent Image Formation in Silver Halides* (World Scientific, Singapore, 1984).
[6] P. W. M. Jacobs, J. Corish, and C. R. A. Catlow, J. Phys. C **13**, 1977 (1980).
[7] B. Dorner, W. von der Osten, and W. Buhrer, J. Phys. C **9**, 723 (1976).
[8] W. G. Kleppmann and W. Weber, Phys. Rev. B **20**, 1669 (1979).
[9] K. S. Song and R. T. Williams, *Self-Trapped Excitons*, 2nd ed. (Springer, Berlin, 1996).
[10] Chun-rong Fu and K. S. Song, J. Phys.: Condens. Matter **9**, 3575 (1997).
[11] G. Rajagopal, R. N. Barnett, and U. Landman, Phys. Rev. Lett. **67**, 727 (1991).
[12] C. R. A. Catlow, J. Corish, J. H. Harding, and P. W. M. Jacobs, Philos. Mag. A **55**, 481 (1987).
[13] C. Kittel, *Introduction to Solid State Physics*, 5th ed. (John Wiley and Sons Inc., New York, 1976).
[14] R. H. Bartram, A. M. Stoneham, and P. Gash, Phys. Rev. **176**, 1014 (1968).
[15] R. D. Zwicker, Phys. Rev. B **18**, 2004 (1978).
[16] R. C. Baetzold and R. S. Eachus, J. Phys.: Condens. Matter **7**, 3991 (1995).
[17] W. G. Kleppmann, J. Phys. C **9**, 2285 (1976).
[18] J. F. Hamilton, in *The Theory of the Photographic Process*, edited by T. H. James (The Macmillan Company, New York, 1977).
[19] E. Clementi and C. Roetti, At. Data Nucl. Data Tables **14**, 177 (1974).